PHYSICS LETTERS A

Phase-locked states and abrupt shifts in Pacific climate indices

CrossMark

David H. Douglass *

Department of Physics and Astronomy, University of Rochester, Rochester, NY 14627, USA

ABSTRACT

Douglass has shown that ENSO index *aNino3.4* contains segments phase locked to subharmonics of the annual solar cycle and also that a set of indices including *aNino3.4* shows abrupt shifts between these phase-locked states. Here, four additional Pacific indices are studied. These five indices show that the Pacific climate system alternates between two regimes: (1) Solar cycle (SOL), (2) Teleconnections (TEL). During SOL each index shows two components that are phase locked to the solar cycle. The first is at the annual cycle, while the second is at a subharmonic of the annual cycle. During TEL abrupt climate shifts occur.

© 2013 Elsevier B.V. All rights reserved.

1. Introduction

Centuries ago South American sailors observed that during some years large increases in coastal tropical Pacific Ocean temperatures occurred in late December [1]. The scientific conclusion is that when El Niño Southern Oscillation (ENSO) effects occur they are phase locked to the annual climate cycle and because the phenomenon does not occur every year the phase locking must be to a subharmonic. Perhaps the first scientific report of subharmonic phase locking between ENSO and the annual cycle was by Bjerknes [2]. He studied the sea surface temperature (*SST*) and the wind velocities at Canton Island (Equatorial mid-Pacific) for the period 1962–1967 and reported: "... *sequence of rhythmic changes of temperature of approximately* 2-*year periodicity.* ... *The main maxima of SST in late* 1963 *and late* 1965 *coincide with the main minima of the* [annual] *easterly wind component*" showing phase locking at subharmonics of the annual frequency. Rasmussen and Carpenter [3] showed that the maximum *SST* anomalies in the central tropical Pacific near 170 W occurred at the end of the calendar year – again indicating phase locking to the annual cycle. Later, Rasmussen, Wang and Ropelewski [4] identified a biennial mode (period 2 years) in *SST* data that was phase locked with the annual cycle. They describe the period 1960–1970 as a well-organized biennial regime. More recently, Douglass [5] (hereafter, D2011) showed that the *aNino3.4* index had distinct time segments phase locked to the second or third subharmonics of the annual cycle. At least ten distinct sequential segments since 1870 were found.

In parallel studies, observations of abrupt changes in climate parameters were being reported. The most studied climate shift is

the Pacific climate shift of the mid-1970s. Ebbesmeyer et al. [6] documented the many aspects of this shift in a study of 40 multidiscipline variables. Many phenomena were proposed to explain this shift. The proposed explanations include: wind by Karspeck and Cane [7]; delay of atmospheric effects by Lindzen and Giannitis [8]; and subsurface anomalies, by Giese, Urizar and Fučkar [9].

Swanson and Tsonis [10] showed that studying correlations between indices can also reveal the occurrence of climate shifts. Using the correlation coefficient between indices they defined a correlation parameter $S(t)$ for more than two indices. They identified maxima in $S(t)$ with climate shifts found in other studies. They reported five maxima (climate shifts) since 1900 using four northern hemispheric indices (*Nino*; Pacific Decadal Oscillation, *PDO*; North Atlantic Oscillation, *NAO*; North Pacific Index, *NPI*).

Douglass [11] (hereafter, D2010) improved the Swanson and Tsonis scheme. He defined a new measure of correlation among climate indices based upon the topological diameter $D(t)$ that was more sensitive. In that study it is the minima in $D(t)$ *that* corresponds to maximum correlation among the indices and which corresponded to the occurrence of known climate shifts. Using a more global set of indices (*Niño3.4*, north and south Pacific SST indices and Atlantic Multidecadal Oscillation, *AMO*) eighteen minima/climate shifts since 1880 were identified including the five found by Swanson and Tsonis.

In Section 2, the data and sources are described. In Section 3 various quantities are defined and in Section 4 the results are given. Discussion and summary are in Sections 5 and 6.

2. Data

All data are monthly values from 1978 onward (the satellite era). There are five Pacific data sets:

* Tel.: +1 585 385 6456.
  E-mail address: douglass@pas.rochester.edu.

Table 1
Descriptions of the five climate indices.

Symbol	Name	Max in climatology	Data range	Coordinates
1 *Nino3.4*	*Nino3.4* (Sea Surface Temperature in Region *SST3.4*)	Apr/May/June	Jan 1950 to 2012	Lat: 5 S to 5 N Long: 120 W to 170 W
2 *SOI*	Southern Oscillation Index. (Surface pressure index between Darwin and Tahiti)	Darwin: June/July/Aug Tahiti: Jul/Aug/Sept	Jan 1951 to 2012	Darwin Long: 131 E; Lat: 12 S Tahiti Long: 150 W; Lat: 18 S
3 *MSU_LT*	Microwave Sounding Unit. Lower Troposphere (atmospheric temperature anomalies in the Tropics)	May/June	Dec 1978 to 2012	Surface to 350 hPa (mean altitude $\sim$2.5 km) Lat: 20 S to 20 N Long: 160 E to 90 W
4 *PDO*	Pacific Decadal Oscillation	Apr/May/June	Jan 1950 to 2012	Pacific. Poleward of 20 N
5 *W3*	*W3* (wind index. Easterly wind velocity at 850 hPa) ($\sim$1.4 km)	May/June/July	Jan 1979 to 2012	Lat: 5 S to 5 N Long: 135 W to 120 W

Table 2
Definitions of various terms.

Definitions of various quantities		
G	Parent geophysical signal	Any of the five time series: *Nino3.4, SOI, MSU_LT, PDO* or *W3*
Filter $\mathfrak{F}$	12-point symmetric moving average "box" digital filter	"removes" the annual signal, harmonics and noise from the G time series
aG	$aG = \mathfrak{F}(G) - \text{trend } \mathfrak{F}(G)$	Contains the ENSO signal
hG	$hG = G - aG$	Contains the annual and harmonics and stochastic noise. Averages of each month are the "climatology"
F_S	Climate forcing originating from the Sun	Causes direct coherent signal in hG and sometimes subharmonic oscillations in aG
SOL	SOL is the regime when the solar forcing F_S dominates teleconnections among the indices	The solar forcing F_S is stronger than those associated with teleconnections
d	$d = \text{acos}(|\text{correlation coefficient between two indices}|)$	Topological measure of teleconnection between two indices
D	Maximum d among more than two indices	Topological teleconnection among many indices
TEL	Teleconnection regime. During this regime F_S is weak or unable to produce subharmonics in aG. As a result, teleconnections among the indices dominate	Minima in topological D (strong correlations) are found in these time segments

Three quantities necessary to characterize phase-locked aG segments of periodicity n-years	
Parity: P	Para parity: if the maxima of aG occurs during April/May/June Ortho parity: if the maxima of aG occurs during Nov/Dec/Jan
Subharmonic number: n	n is the number of annual oscillations during one oscillation of aG
Equivalent substates: **mod index**	The n equivalent substates are indexed by *mod index* = annual (mod aG), where the mod index can take on one the values $[0, 1, \ldots, n-1]$

(1) *Nino3.4*. These data are sea surface temperature (*SST*) anomalies from tropical Pacific Region 3.4 [12].
(2) *SOI*. These data are Pacific tropical pressure anomalies between Darwin Australia and Tahiti [12].
(3) *MSU_LT*. These data are temperature anomalies of the Pacific lower tropical troposphere [13].
(4) *PDO*. These data are SST temperature anomalies north of 20 N [14].
(5) *W3*. These data are easterly values of tropical wind at atmospheric pressure 850 hPa (lat: 5 S to 5 N; long: 175 W to 120 E). [12].

Table 1 gives a more complete description of these five indices.

3. Definitions and background material [D2010, D2011] (Table 2)

3.1. Climate time series contain two signals of interest

The study of many geophysical phenomena starts with a parent signal G (any of the five climate indices) that contains a signal of interest N that shows ENSO effects plus a seasonal signal X at frequency of 1.0 cycles/year and its harmonics. For example, in D2011 the parent signal is *SST3.4*, the signal of interest is labeled N_L containing the ENSO effects and the seasonal signal is labeled N_H.

The first task of many studies is to separate X from G to obtain N. In D2011 it is shown that a

12-month moving average filter $\mathfrak{F}$ (1)

applied to G separates out X. It was also shown in some detail that X should be considered to be an essential component of the ENSO phenomena and retained.

Two climate indices. The filter $\mathfrak{F}$ is applied to the time series G to create a "season free" anomaly index

$$aG = \mathfrak{F}(G) - \text{trend } \mathfrak{F}(G) \qquad (2)$$

where the trend, over a range of G, removes long term secular effects. This signal contains the familiar ENSO phenomena. Secondly, a "high frequency" index is defined,

$$hG = G - \mathfrak{F}(G) \qquad (3)$$

that contains the coherent signal at 1.0 cycles/year and harmonics plus noise. The coherent signal is obviously of solar origin.

The ENSO index given by Eq. (2) is a direct challenge to the commonly used "climatology" method of removing the seasonal effect. The climatology method consists of: (1) Creating a set of

"climatology" values that are averages for each month of the year from the G time series over a specified range; these 12 climatology values actually derive from the coherent annual component of hG. (2) This ENSO index is defined as G minus the appropriate climatology value. In D2011 it was shown that in the case of *Nino3.4* this climatology scheme fails to remove all of the seasonal effect while the 12-month filter method does remove it. It was also shown that filter $\mathfrak{F}$ applied to this climatology generated index gives values very close to aG.

3.1.1. Index hG

In D2011 the delayed autocorrelation calculation for *hNino3.4* showed a sustained oscillation of period of 12 months. That the oscillations are sustained implies that there is an external forcing. From the fact that the frequency is 1.0 cycles/year further implies that the external forcing is of solar origin. All five indices in this study will be shown below to have the same sustained oscillation frequency of 1.0 cycles/year.

3.1.2. Index aG

Defining phase-locked time-segments of aG [D2011]. Observation of certain time-segments of aG show a periodicity that is $n \cdot 12$ months, where $n = 2, 3, 4$ ($n = 1$ has been removed by the 12-month filter).

The description of the phase-locked state requires three discrete quantities.

(1) Parity.

It must be true that the climatology calculated from either G or hG has a maximum during certain quarters of the year. For all five of the indices considered in this Letter this was determined to occur during May/June/July (MJJ). Next, if there are coherent time segments of aG for which the maxima occur at multiples of 12-months then there must be a month for which this maximum is observed. For *Nino3.4*, two possibilities occurred. They were Nov/Dec/Jan and May/Jun/Jul (MJJ). The two possibilities found were either in phase or out of phase with the climatology. The terminology for these two possibilities was defined:

Ortho parity: if the maxima of aG occur during NDJ. (4a)

Para parity: if the maxima of aG occur during MJJ. (4b)

(2) Subharmonic number n.

This is the number of annual oscillations of aG during one oscillation of hG.

(3) Equivalent substates: mod index.

If aG is phase locked to the nth subharmonic of the annual frequency, then there are n annual oscillations to one of N_L and thus there are n equivalent maxima. The n equivalent substates are indexed by *mod index*, where the *mod index* has the values $[0, 1, \ldots, n - 1]$. For example, a segment with period 3 years has three equivalent mod states that can be indexed by 0, 1 and 2.

Thus, the characterization of a phase-locked state requires three discrete indices: parity, subharmonic number and mod index.

3.2. Determination of the periodicity and parity of a time segment of aG

One wants to determine if a particular time segment of aG has a periodicity of $n \cdot 12$ months. The value of n of the candidate time

segment can be quantitatively ascertained from the autocorrelation function of the time segment vs. lag time τ, which will have a maximum at τ values of 24, 36, 48, etc., months. By adding or subtracting data values to the time segment until the maximum in the autocorrelation function occurs precisely at 24, 36, 48 months one determines the beginning and end dates of a phase-locked segment with a relative accuracy of several months.

The parity is determined by noting whether the month of the occurrence of the maxima in the segment are in phase or out of phase with the climatology. For example, the climatology of *Nino3.4* has its largest value during MJJ while the maxima during 2001–2008 (the coherent segment #10 of period 2-years) has their maximum during NDJ. Thus, the parity of this segment is "ortho". A similar analysis of segment 8 from 1985–1990 (period three years) shows that the parity is "para". States of the same parity and periodicity can have different substates. Again from *aNino3.4*, one finds examples of all three mod indices in the set of segments with the same parity and with periodicity 3 years [D2011].

3.3. Teleconnections and climate shifts

Ångström [15] coined the term "teleconnections": *The existence of changes of great extension in some properties: … affects the weather and … in fact often in a different way in different localities.* In application, he defined teleconnections to mean the correlation coefficient between two climate variables. It is useful to explain in geometric terms the meaning of this coefficient. The correlation coefficient $\Phi_{ij}(t)$ is calculated between two climate time segments over a symmetric time window t_W. To calculate the coefficient, the elements in each time segment are considered as components of a vector of length t_W. Unit vectors are then constructed. The correlation coefficient is the inner product of the two unit vectors, which is the cosine of the angle between the two unit vectors. The value of the time window t_W must be large enough to average out the ENSO effects that are typically 3 to 5 years in duration. The value used in this Letter will be 7 years (84 months) as was used by Swanson and Tsonis et al. and in D2010.

Teleconnection between two indices. In D2010 it was pointed out that the correlation coefficient did not satisfy certain desirable mathematical conditions and a new measure of teleconnection between two climate variables was defined. The new measure between two climate indices (i and j) from a set of N indices was defined and named the topological "distance" $d_{ij}(t)$

$$d_{ij}(t) = \cos^{-1}\big(\big|\phi_{ij}(t)\big|\big). \tag{5}$$

This distance is the spherical angle between the two unit vectors on the unit sphere and is bounded between 0 and 90 degrees. Towsley, Pakianathan and Douglass [16] showed that this distance satisfies the conditions

1. $d_{ij} \geqslant 0$ (non-negativity), (6a)

2. $d_{ij} = d_{ji}$ (symmetry), (6b)

3. $d_{ik} + d_{kj} \geqslant d_{ij}$ (triangle inequality) ($i \neq k \neq j$), (6c)

which is sufficient for the set I_0 of indices together with the pairwise distances d_{ij} between these indices to form a metric space, (I_0, d_{ij}). Simultaneous climate shifts occurring in two indices (i and j) are found in those time segments for which there is a minimum in d_{ij}.

Teleconnections among more than two indices. How can the teleconnection be defined if there are more than two indices? This was answered in D2011. Having a metric space (I_0, d_{ij}) allows

the topological diameter D [17] to be used as a measure of the teleconnection among the members of the set I_0. The topological diameter $D(t)$ is defined as

$$D_{I_0}(t) = \max\big[d_{ij}(t) \,\big|\, i, j \in I_0; \; i \neq j\big], \qquad (7)$$

where i and j are any of the indices in the set I_0. Thus, D selects the largest angle (d_{ij}) among the $N(N-1)/2$ members of the set I_0. D2010 showed that minima in $D(t)$ corresponded to known climate shifts. Eighteen such minima since 1870 were reported. Towsley et al. (2011) showed that the topological diameter D was the first in a hierarchy of more sensitive definitions. Next is the area A involving triplets of points on the unit sphere. Area A was demonstrated to be more sensitive by studying the same set of indices used in D2011; all of the minima found in D2010 were found to be stronger. In addition, other less strong minima in A were found that corresponded to ends and/or beginnings of coherent segments subsequently reported in D2011.

3.4. The 1D nonlinear oscillator

If a linear oscillator of intrinsic frequency f_0 is driven by a forcing F at frequency f_F, there is a direct response, N_1, at f_F – in phase if $f_F < f_0$ and out of phase if $f_F > f_0$. If the oscillator is nonlinear then, simultaneously, additional oscillations may occur at subharmonics of f_F. Stoker [18] explicitly considers the response $N_{1/3}$ at $f_F/3$. The conditions for $N_{1/3}$ to exist involve the nonlinear coefficient, the amplitudes and the difference between $f_F/3$ and f_0 as well as other quantities. The conditions yield a lower and an upper bound in parameter space. Outside of these bounds there are no solutions for $N_{1/3}$. A solution, if generated, will terminate abruptly if variation of the amplitudes or nonlinear parameter causes the conditions not to be satisfied.

The results below will be compared to this example of the 1D nonlinear oscillator.

4. Analysis of data

The aG and hG components of the five Pacific data sets were calculated.

### 4.1. Indices hG: the annual component

The delayed autocorrelation of hG for all five indices showed a sustained oscillation of period of 12 months. Next, the maxima of the annual component of each of the five hG data sets was determined to occur during May/June/July (MJJ) and a minimum during Nov/Dec/Jan (NDJ). The observation that the date range is the same for all five indices suggests a single explanation that will be discussed below.

4.2. Indices aG

Subharmonic phase locking to the annual cycle. When subharmonics of the solar cycle are observed the climate system is defined as being in a regime labeled SOL. Figs. 1a, b show the aG times series for each of the five climate indices. Oscillations characteristic of the ENSO phenomena are clearly evident. The El Niño of 1997–1998 is circled in red to show commonality. Each index was studied for phase-locked segments of period $n \cdot 12$ months, where $n = 2, 3$ or 4. An easy segment to find is from 2001–2008 which shows a 24-month oscillation in all five indices. The beginning and end of a candidate time segment for all was found by the autocorrelation method with a relative accuracy of several months. Five of these phase-locked time segments were identified. The thick red horizontal segmented line shows the duration and
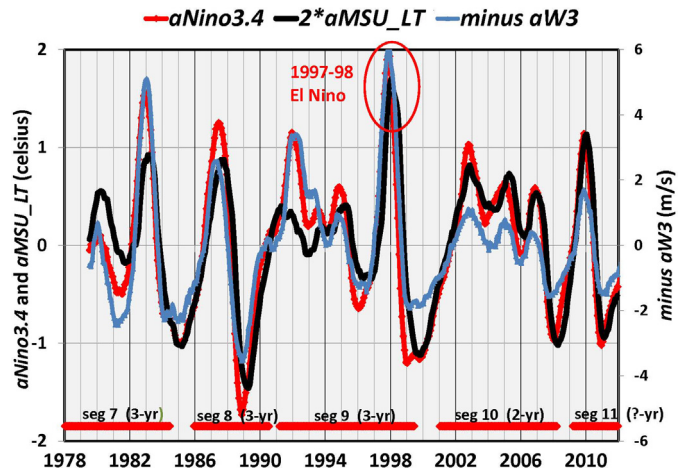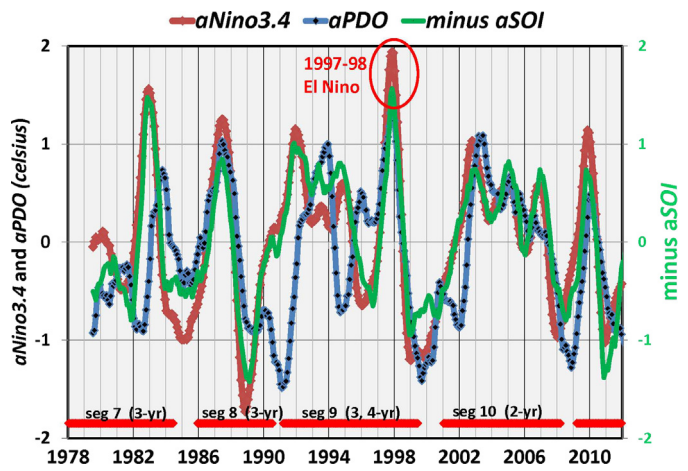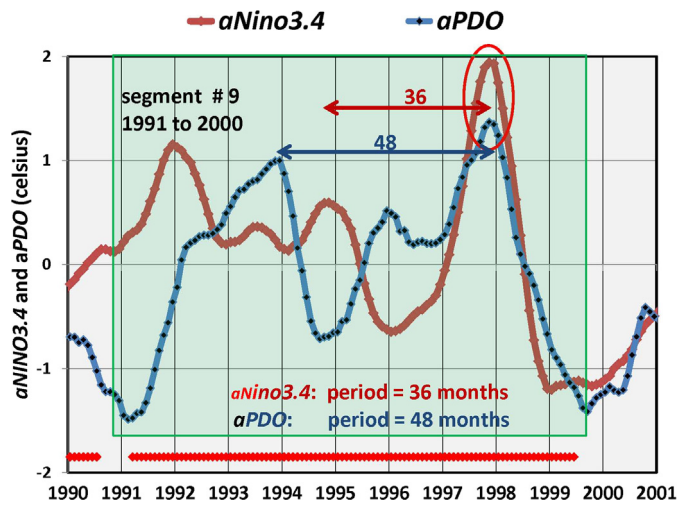
Fig. 1. The El Niño of 1997–98 is indicated by a red circle. Horizontal red bars show the duration of subharmonic phase-locked time segments. (a) *aNino3.4, aMSU* and *aW3*. Horizontal red bars show the duration of subharmonic phase-locked time segments (S5, S6, S7, S8, S9, S10 and S11) reported in D2011. (b) *aNino3.4, aPDA* and *aSOI*. Horizontal red bars show the duration of subharmonic phase-locked time segments (S5, S6, S7, S8, S9, S10 and S11) reported in D2011. (c) *aNino3.4* and *aPDO*. Horizontal red bars show the duration of subharmonic phase-locked time segment S9. (For interpretation of the references to color in this figure legend, the reader is referred to the web version of this Letter.)

Table 3
Properties of various time segments.

TEL regime		SOL regime										
Minimum of D		Phase-locked state (See *D2010* and text)				Begin/End Dates (uncertainty ± 6 months)						
Index # (see note a)	Begin/End Dates (±6 months)	Seg ment #	Parity	Period (years)	Mod index	(1) *aNino3.4*	(2) *aSOI*	(3) *aMSU_LT*	(4) *aPDO*	(5) *aW3*	Average Range	
				subharmonic state								
		7	O	3	0	Jan 1975 to Jun 1984	Jan 1975 to Jun 1984	No data	Dec 1975 to Jan 1984	No data	Jan 1975 To Jan-Jun 1984	
16a 17	Apr 1984 Oct 1986											
		8	P	3	0	Dec 1985 to Oct 1990	Dec 1985 to Oct 1990	Jan 1886 to Nov 1990	Jul 1985 to Oct 1990	Jul 1985 to Oct 1990	Jul 85-Jan 86 To Oct 90-Nov 90	
17a	Jan 1990 Feb 1990											
		9 (see note b)	O	PDO = 4	0	Jan 1991 to July 1999	Jan 1991 to July1999	Dec 1990 to July 1999	Dec 1990 to May 1999	Jan 1991 to July 1999	Dec 90- Jan 91	
			O	Others = 3	0						May 99- Jul 99	
18 19	Apr 2000 Feb 2002											
See Note c		10	O	2	0	May2001 to Mar 2008	May2001 to Mar 2008	May2001 to Mar 2008	Dec 2000 to Mar 2008	May 2001 to Mar 2008	Dec 00-May 01 To Mar 08-Mar 08	
20	Mar 2008 Aug 2008											
		11	O	3 (?)	0	Sep 2008 to ?	Sep 2008 to ?	Jan 2009 to ?	Jan 2008 to ?	Sep 2008 to ?	Jan 08-Jan 09 to ?	

Note a: The *D* index numbers come from D2011 and Towsley et al. Index #19, #20 are new.
Note b: In this interval of 8+ years, *Nino3.4* shows about three cycles of period 3-years, while *PDO* shows about two cycles of period four years.
Note c: Minimum in *D* at 2006 is associated with *dPDO*.

periodicity of each segment. The labeling 7, 8, 9, 10, and 11 continues the scheme defined in D2011.

The various states, duration, periodicities and parities are listed in Table 3. They are the same as previously found for *aNino3.4* with one exception. That exception is for *aPDO* during phase-locked segment #9 (1991 to 1999). Fig. 1c shows *aPDO* along with *aNino3.4* for comparison. This figure shows the remarkable result that during this interval that both *aPDO* and *aNino3.4* are phase locked to the common annual cycle but with different periodicities: *aPDO* shows about two cycles of 4-yr period while *aNino3.4* shows about three cycles of 3-yr period.

Intervals of high correlation (small D). From above, time segments of *aG* with large teleconnections (small topological *D*) indicate the climate system is in a new regime labeled TEL.

The topological diameter *D(t)* among the five *aG* indices was calculated and is shown in Fig. 2. Six minima were found and are indicated by black arrows (1984, 1986–1987, 1990, 2001, 2002, and 2008–2009). The first four are the same as was reported by D2011 and by Towsley et al. [16]. The last two are new and will be discussed below. Also shown by thick horizontal red bars are the range of duration of the phase-locked SOL segments.

5. Discussion

The observations show that *G* (any of the five indices) has two components. The first, *hG*, contains a coherent signal at 1.0 cycle/year of solar origin. The second, *aG*, shows time segments that alternate successively between two regimes: (a) SOL: A solar cycle dominated regime. (b) TEL: A regime where teleconnections
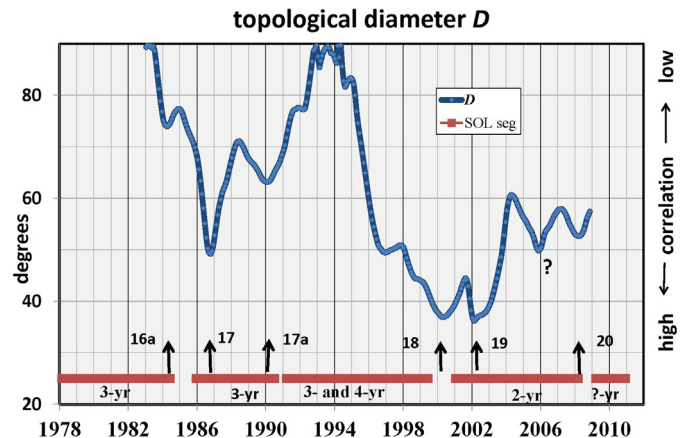
Fig. 2. Topological diameter *D* (blue). Horizontal red bars show the duration of subharmonic phase-locked time segments (S7, S8, S9, S10 and S11). The black arrows are minima in *D*; the index numbers are the same as in D2010. The minimum #19, 20 are new. (For interpretation of the references to color in this figure legend, the reader is referred to the web version of this Letter.)

among the indices are strong and where minima in topological *D* indicate climate shifts.

5.1. Existence of a solar forcing F_S

Observation of sustained oscillations in the autocorrelation function of *hG* means that there must be an external forcing F_S to sustain the oscillations. That the period of the oscillations is 1.0 cycle/year indicates that the forcing is of solar origin. A further

observation is that the maxima in hG of all five indices occur during May/June/July (MJJ) means that there are not five different solar forcings but only one.

5.2. The SOL regime

During this regime the solar forcing F_S dominates the teleconnection interactions among the indices. F_S causes hG which is phase locked directly to the solar cycle. In addition, F_S may cause a second response, aG, at subharmonics which are also phase locked to the solar cycle. The appearance of the subharmonic oscillations indicates that nonlinear effects are present and important. The beginning and ending dates of these SOL time segments are nearly the same for all indices. In addition, the particular subharmonic state of each index can be different.

In D2011, eleven SOL time segments in $aNino3.4$ between 1870 and 2010 were enumerated. The present investigation begins in 1978 and finds five SOL time segments that correspond to segments 7, 8, 9, 10, and 11 of D2011. See Table 3.

5.3. The TEL regime

It is observed that at some point in time a SOL regime ends abruptly and a new regime, the TEL regime, begins. During the TEL regime the teleconnections among the indices are stronger than the nonlinear solar forcing effects. The beginning of the TEL regime is signaled by a minimum in the topological diameter D.

The dates of the minima in D are in general agreement with values reported in prior studies. The last two minima at 2002 and 2008–2009 are new. (Note: the enumeration of the various minima in D reported in D2010 and Towsley et al. [16] is adopted and extended in this study.)

At some point in time after the beginning of a TEL regime (several months to several years) the TEL interactions become weaker relative to the SOL interactions and the climate system again abruptly changes to a new SOL regime.

5.4. What causes the abrupt changes in state?

The abruptness of the beginnings and/or ends of phase-locked time segments suggest impulses to the climate system. El Niños can be ruled out because the most recent large El Niños (1973–74, 1983–84 and 1997–98) do not correspond to any climate shifts. A more likely possibility is similar to that which occurs for the 1D nonlinear oscillator. The subharmonic oscillations are stable only between lower and upper limits of a parameter that depends on the nonlinearity and the amplitudes. If during a subharmonic oscillation these conditions are not satisfied the oscillation will end abruptly. A similar argument can be made for the initiation of a subharmonic oscillation. This possibility will be explored in a later paper.

5.5. The El Niño of 1997–1998

The El Niño of 1997–98 was the largest such event during the last century. No satisfactory explanation has been offered. It is noted that El Niños are "merely" the positive portion of an oscillation in a subharmonic phase-locked time segment. Also, the El Niño of 1997–98 occurs in time segment #9 in which $aNino3.4$ has periodicity 3-years and $aPDO$ has periodicity 4 years. In addition, both have their maxima during Nov/Dec/Jan (NDJ). Fig. 1c shows that during this time segment that the maxima in the two time series coincide during 1997–98. Even though the northern and central Pacific are weakly coupled, this coincidence of their maxima in SST anomaly may be part of the explanation for a very large amplitude El Niño.

5.6. Climate predictions

Predicting future climate phenomenon depends on (1) knowledge of the past and (2) an extrapolation to the future. The common assumption of continuity of the derivatives of relevant climate variables cannot be used. In particular, extrapolating a slope into the future should not be done. This is especially true because of the climate shift during 2008–2009. What can be done? One could reasonably expect the future would have climate shifts similar to the past. In the case of $aNino3.4$ the past showed at least 18 climate shifts since 1870. From the fact that the trend of $Nino3.4$ with its many climate shifts was close to zero, one may infer that climate shifts on average act to bring the climate system toward equilibrium. In fact, it may be true that if the climate system becomes too far out of equilibrium that a climate shift must occur.

6. Conclusions

This study shows that for the Pacific climate system there are two regimes:

Solar cycle (*SOL*). During this regime the Sun is the "pacemaker" regulating when maxima and minima occur. In this regime an external forcing F_S of solar origin is dominant and causes a direct response hG at 1.0 cycles/year. In addition, F_S may also cause a response aG at subharmonics if certain conditions involving nonlinearities are satisfied. When subharmonics are observed the states may be different. For example, during 1991–1999 index $aPDO$ showed phase locking of 4-yr period while the others showed phase locking of 3-years. The last complete SOL time segment was from 2001 to 2008 in which all indices were in a phase-locked state of period 2 years. At some point in time a perturbation occurs and the climate system changes abruptly to

Teleconnections (*TEL*) *regime*. During this regime, the nonlinear interactions that dominate during a SOL regime are "turned off" or are weaker than the teleconnection interactions among the components of the Pacific climate system. The TEL regime is signaled by minima in the topological diameter D which correspond to climate shifts. The last two climate shifts occurred during 2001–2002 and 2008–2009.

Acknowledgements

References

[1] M.H. Glantz, Currents of Change, Cambridge University Press, Cambridge, UK, 2001.
[2] J. Bjerknes, Technical report. ONR contract No. N0014-69-A-0200-4044 NR 083-287, 1969.
[3] E. Rasmusson, T. Carpenter, Monthly Weather Rev. 110 (1982) 354.
[4] E. Rasmusson, X. Wang, C. Ropelewski, J. Marine Syst. 1 (1990) 71.
[5] D.H. Douglass, Phys. Lett. A 376 (2011) 128, http://dx.doi.org/10.1016/jphysleta.201110.042 (pdf here).
[6] C.C. Ebbesmeyer, D.R. Cayen, D.R. McLain, F.H. Nichols D.H, Peterson, K.T. Redmond, in: J.L. Betancourt, V.L. Tharp (Eds.), Proceedings of the 7th Annual Pacific Climate (PACLIM) Workshop, April 1990, California, 1991.
[7] A.R. Karspeck, M.A. Cane, J. Phys. Oceanogr. 32 (2002) 2350, http://dx.doi.org/10.1175/1500485(2002)j032<TPCSIA>2.o.CO.
[8] R.S. Lindzen, C. Giannitis, Geophys. Res. Lett. 29 (2002), http://dx.doi.org/10.1029/2001GL014074.
[9] B.S. Giese, S.C. Urizar, N.S. Fučkar, Geophys. Res. Lett. 29 (2002), http://dx.doi.org/10.1029/2001GL013268.
[10] K. Swanson, A. Tsonis, Geophys. Res. Lett. 36 (2009) L06711, http://dx.doi.org/10.1029/2008GL037022.

[11] D.H. Douglass, Phys. Lett. A 374 (2010) 4164, http://dx.doi.org/10.1016/j.physleta.2010.08.025 (pdf here).

[12] NOAA/CDC, web site at http://www.cpc.ncep.noaa.gov/data/indices/, 2012.

[13] UAH, 2012, data kindly furnished by John R. Christy.

[14] PDO, data at http://jisao.washington.edu/pdo/PDO.latest, 2012.

[15] A. Ångström, Geogr. Annal. 17 (1935) 242.

[16] A. Towsley, J. Pakianathan, D.H. Douglass, ISRN Appl. Math. 2011 (2011) 323864, http://dx.doi.org/10.5402/2011/323864 (pdf here).

[17] J.R. Munkres, Topology, Prentice Hall, 2006 (Section 20).

[18] J.J. Stoker, Nonlinear Vibrations, Interscience, 1950.